Talanta 130 (2014) 103–107

Contents lists available at ScienceDirect

Talanta

journal homepage: www.elsevier.com/locate/talanta

# A novel donor–acceptor receptor for selective detection of $Pb^{2+}$ and $Fe^{3+}$ ions

Kamlakar P. Nandre [a,b], Avinash L. Puyad [c], Sheshanath V. Bhosale [d,*], Sidhanath V. Bhosale [a,*]

[a] Polymers and Functional Materials Division, CSIR-Indian Institute of Chemical Technology, Hyderabad-500 007, Telangana, India
[b] Department of Organic Chemistry, School of Chemical Sciences, North Maharashtra University, Jalgaon-425001, India
[c] School of Chemical Sciences, SRTM University, Nanded-431 606, Maharashtra, India
[d] School of Applied Sciences, RMIT University, Melbourne, VIC-3001, Australia

ARTICLE INFO

*Article history:*
Received 1 June 2014
Received in revised form
26 June 2014
Accepted 27 June 2014
Available online 5 July 2014

*Keywords:*
Sensor
Colorimetric
Fluorescence
$Pb^{2+}$ and $Fe^{3+}$ cations
UV–vis absorption

ABSTRACT

An efficient and highly selective colorimetric and fluorescent receptor DTPDA has been synthesized for sensitive detection of $Pb^{2+}$ and $Fe^{3+}$ cations. The sensor DTPDA produces a facile, cost-effective and naked eye sensing platform to determine trace amounts of $Pb^{2+}$ and $Fe^{3+}$ metal ions by complexation with pendent S-termini of thiophenes, which commonly coordinates to central N-termini of pyridine.



## 1. Introduction

The development of highly sensitive fluorescence receptors for the selective recognition of heavy metal ions and transition metals has been inspiring the scientific community for the past few years as a result of concern for human health and environmental safety [1–5]. Among them, lead is one of the most highly toxic metal cations. It is widely spread through the environment and causes serious adverse effects to human health, particularly in children where it causes memory loss, anaemia, mental retardation, muscle paralysis and irritability [6]. According to the World Health Organisation (WHO), 10 mg $L^{-1}$ is the permissible limit of lead for drinking water [7]. On the other end of the spectrum, iron is one of the most essential trace element in the human body, is present in many enzymes and proteins and acts as cofactor for many cellular metabolism reactions [8]. It plays an important role in the transportation of oxygen to all tissues, in the form of haemoglobin. Both its deficiency and excess in human body can results in various pathological disorders [9] with iron transporting, storage and balance [10]. A literature survey reveals that various chemosensors have been developed for the selective detection of either $Pb^{2+}$ or $Fe^{3+}$ metal ions [11–17]. However, there is still a growing demand to develop a chromogenic receptor for the highly selective and sensitive detection of these both cations.

Molecules with triphenylamine based donors and thiophene acceptors have received a lot of attention due to their wide range of applications in organic photovoltaics (OPVs) [18], organic light-emitting diodes (OLEDs) [19], organic light-emitting transistors (OLETs) [20], organic solar cells (OSCs) [21], fluorescent sensors [22,23], and electro-polymerisation [24]. The donor and acceptor groups in these molecules are connected skeletally through linear $\pi$-conjugated systems, which gives rise to their isotropic, optical and charge transporting properties. Motivated by such significant applications of donor–acceptor synthetic systems and how they can overcome the emission quenching nature and interfering effect of other cations, we are interested in developing a new fluorescent receptor for cation sensing.

## 2. Experimental section

### 2.1. General information and materials

All reagents were purchased from Sigma Aldrich Chemical Co. and were used as without further purification. All solvents were received from commercial sources and purified by standard

* Corresponding authors.
*E-mail addresses:* bhosale@iict.res.in (S.V. Bhosale), sheshanath.bhosale@rmit.edu.au (S.V. Bhosale).

http://dx.doi.org/10.1016/j.talanta.2014.06.064
0039-9140/

methods. For all spectroscopic studies, acetonitrile of HPLC grade were used. $^{1}H$ and $^{13}C$ NMR spectra were recorded on ADVANCE 300 and 75 MHz NMR spectrometer respectively using TMS as internal standard and $CDCl_3$ as the solvent. Mass spectrometric data were obtained by electron spray ionization (ESI-MS) technique on an Agilent Technologies 1100 Series (Agilent Chemistation Software) mass spectrometer. High-resolution mass spectra (HRMS) were obtained by using ESIQTOF mass spectrometry. FTIR spectra were obtained on a Perkin Elmer FT-IR 400 spectrometer.

### 2.2. UV–vis spectroscopic studies

UV–vis spectra were recorded in a Shimadzu 2450 UV–vis spectrometer in 1 cm path length cuvette. A stock solutions of **DTPDA** ($8\times10^{-5}$ M) and various metal perchlorate salts ($2\times10^{-4}$ M) were prepared in acetonitrile and allowed to equilibrate at room temperature for 2 h before spectral measurements.

### 2.3. Fluorescence spectroscopy

Fluorescence emission spectra were recorded in a Horiba Jobin Yvon FluoroMax®-4 –Spectrofluorometer. All experiments were performed in a quartz cell with a 1 cm path length with 350 nm excitation wavelength. Solution preparation is in similar manner as mentioned in UV–vis study.

### 2.4. Density functional theory (DFT)

To determine the most stable energy conformation of sensor DTPDA, three possible conformations (Fig. S15) are optimized by using hybrid density functional B3LYP with basis set 6–31+G(d). Frequency calculations are carried out at the same level of theory to ensure that the conformations are real structures. After comparing the energies of three possible conformations the DTPDA1 is found to be the most stable (Table S1). Optimized geometrical parameters (bond length in Å and angle in Deg) of three possible conformations obtained at B3LYP/6–31+G(d) level of theory are given in Table S2.

### 2.5. Synthesis of derivatives

Synthesis of (*E*)-3-(4-(diphenylamino)phenyl)-1-(thiophen-2-yl)prop-2-en-1-one (**2**)

To a mixture of 4-(diphenylamino) benzaldehyde [25] (**1**) (2.0 g, 0.007 mol) and 2-acetyl thiophene (0.9 g, 0.03 mol) in ethanol (50 mL), a solution of potassium hydroxide (5%, 50 mL) was added slowly. The mixture was stirred for 24 h. The precipitated solid was filtered, washed with water, dried, and recrystalized from ethanol gives **2** (2.56 g, 92%), as a yellow solid. $^{1}$NMR (300 MHz, $CDCl_3$) $\delta$ (ppm): 7.83 (d, 1*H*, *J*=3.9 Hz), 7.64 (d, 1*H*, *J*=5.4 Hz), 7.48 (d, 2*H*, *J*=8.7 Hz), 7.33–7.01 (m, 15*H*); $^{13}$C NMR (75 MHz, $CDCl_3$) $\delta$ (ppm): 181.9, 146.7, 143.8, 133.2, 131.2, 129.7, 129.4, 129.1, 128.0, 125.4, 124.1, 122.6, 121.4, 118.9, 127.6. ESI-MS (*m*/*z*): 382 $[M+H]^+$, calcd. for $C_{25}H_{19}NOS$=382.1437, found=382.1264.

Synthesis of 4-(2,6-di(thiophen-2-yl)pyridin-4-yl)-*N*,*N*-diphenylaniline (**DTPDA**)

An equimolar amount of compound **2** (2.0 g, 0.005 mol) and *N*-[1-oxo-2-(2-thienyl)ethyl]-pyridium iodide [26] (**3**) (3.0 g, 0.008 mol) was heated under reflux condition for 12 h in the presence of ammonium acetate (5.0 g, 0.648 mmol) and glacial acetic acid (15 mL). After the reaction mixture was maintained at room temperature overnight, ice cold water (30 mL) was added to it, the obtained precipitated was filtered, wash with water, dried and purified by column chromatography to afford the probe DTPDA (0.79 g, 31%) as faint green solid. $^{1}$NMR (300 MHz, $CDCl_3$) $\delta$ (ppm):7.69 (d, 2*H*, *J*=3 Hz), 7.66 (s, 2*H*), 7.57 (d, 2*H*, *J*=8.4 Hz), 7.40 (d, 2*H*, *J*=4.8 Hz), 7.28 (t, 4*H*, *J*=7.5 Hz), 7.19–7.06 (m, 10*H*); $^{13}$C NMR (75 MHz, $CDCl_3$) $\delta$ (ppm): 152.4, 149.3, 148.9, 147.2, 144.9, 131.3, 129.3, 127.8, 127.6, 124.8, 124.6, 123.5, 122.9, 114.3. ESI-MS (*m*/*z*): 487 $[M+H]^+$, calcd. for $C_{31}H_{23}N_2S_2$=487.1297, found=487.1283.

## 3. Results and discussion

Herein, we designed a novel receptor based on donor–acceptor strategy, which possesses triphenylamine as a donor and *bis*-thiophenes appended to a pyridine unit as an acceptor moieties. The fluorescent probe 4-(2,6-di(thiophen-2-yl)pyridin-4-yl)-*N*,*N*-diphenylaniline (**DTPDA**) was synthesized in two steps (Scheme 1, for detail see ESI†), in the first step reaction of **1** with 2-acetyl thiophene in KOH in ethanol gives compound **2** in 92% yield and in the final step reaction of **2** with *N*-[1-oxo-2-(2-thienyl)ethyl]-pyridium iodide in acetic acid in the presence of ammonium acetate produced **DTPDA** target molecule in 31% yield.

The plausible mechanistic pathway is as depicted in Scheme 1. A synthetic methodology to fabricate pyridine derivatives based on ring closure of 1,5-diketo-derivatives was reported by Kröhnke [27]. Triphenylamine monoaldehyde **1** and 2-acetylthiophene undergoes base mediated aldol-condensation that yields the α,β unsaturated ketone **2**. In the second step, **2** reacts with pyridinium salt of acetylthiophene **3** afforded 1,5-diketo-derivative **4** *via* Michael addition. The obtained derivative was not isolated. In third step, 1,5-diketo-derivative **4** undergoes in situ ring closure reaction in the presence of ammonium acetate leading to the target molecule **DTPDA** [28,29].

### 3.1. Density functional theory (DFT) calculations

To gain insight the electronic structure of receptor molecule **DTPDA**, we performed density functional theory (DFT) calculations. The results of calculations reported in this work were obtained using the Gaussian 09 ab initio/DFT quantum chemical simulation package [30]. The lowest energy conformation of receptor molecule **DTPDA** was determined by gas phase optimization of all possible conformations (Fig. S15, for detail see ESI†)) using hybrid density

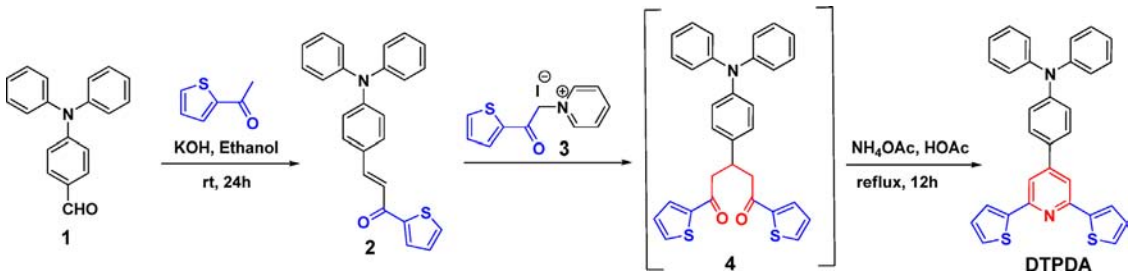


**Scheme 1.** Synthesis of **DTPDA** receptor.

functional B3LYP with basis set 6–31+G(d). Frequency calculations were carried out at the same level of theory to ensure that **DTPDA** has all real (positive) frequencies. Based upon the obtained molecular geometry of **DTPDA**, the frontier molecular orbitals HOMO and LUMO were calculated at the same level of theory and generated by using Avogadro software (Fig. 1) [31,32]. The HOMO (−5.40 eV) electron cloud is on the triphenylamine part and LUMO (−1.73 eV) electron cloud is spread over from the two-thiophenes to the nitrogen of the triphenylamine part of receptor molecule. The calculated energy gaps i.e. HOMO–LUMO gap (HLG) for receptor molecule is 3.67 eV. Thus, for **DTPDA**, the ICT transitions predominantly involve the triphenylamine donor and *bis*-thiophenes appended pyridine as an acceptor end.

### 3.2. UV–vis absorption and fluorescence spectroscopy

UV–vis and fluorescence spectroscopy of **DTPDA** were studied at room temperature in acetonitrile. The UV–vis absorption spectra of **DTPDA** exhibited four major peaks at 200, 251, 292 and 352 nm. The absorption band at 352 nm may be appeared due to a spin-allowed intramolecular charge transfer (ICT) band ($\pi$–$\pi^*$ transition) [33,34]. Furthermore, the cation binding properties of **DTPDA** were investigated using UV–vis spectroscopic measurements. In this regard **DTPDA** ($8\times10^{-5}$ M) was treated with 10 equiv. of each individual cations such as $Fe^{3+}$, $Ag^{+}$, $Ba^{2+}$, $Ca^{2+}$, $Cu^{2+}$, $Hg^{2+}$, $Mg^{2+}$, $Mn^{2+}$, $Pb^{2+}$, $Ni^{2+}$, $Zn^{2+}$ and $Cd^{2+}$ as their perchlorate salts in acetonitrile (Figs. 2 and S2). UV–vis absorption spectrum in the presence of 10 equiv. of different individual cations ($2.0\times10^{-4}$ M) reveals the peaks of **DTPDA** were not shifted by any of the cations except $Pb^{2+}$ and $Fe^{3+}$. The absorption band of **DTPDA** at 250 nm, 295 nm and 350 nm decreased in intensity with $Pb^{2+}$ ion and generation of new absorption peak at $\lambda_{max}$=453 nm with $Fe^{3+}$ ion, suggesting a selectivity towards only $Pb^{2+}$ and $Fe^{3+}$ ions.

We further investigated the changes in the UV–vis absorption spectra of receptor **DTPDA** upon addition of increasing amount of $Pb^{2+}$ ions (0 equiv. to 10 equiv.) to the acetonitrile solution. As shown in Fig. 3a, upon addition of increasing amount of $Pb^{2+}$ ions shows a decrease in intensity of absorption bands at 250 nm, 295 nm and 350 nm, indicating that the receptor is available for selective detection of Pb(II). Notably, as shown, such absorbance response of receptor **DTPDA** towards other cations was not observed for these peaks. Furthermore, we observed that the addition of $Pb^{2+}$ leads to an increase in absorption at 209 nm. The plot of linear increase in absorption intensity at 209 nm with number of equivalent of $Pb^{2+}$ indicates 1:1 stoichiometry for **DTPDA**.$Pb^{2+}$ complex (Fig. S3). The bathochromic shift was associated with a visual detection in the change in color from colourless to the dark orange of the resulting solution (Fig. S1) and clearly indicates binding of $Pb^{2+}$ to the **DTPDA** receptor.

The binding of $Pb^{2+}$ with **DTPDA** was also investigated by fluorescence spectroscopy techniques. Upon excitation at $\lambda_{ex}$= 350 nm, the fluorescence spectrum shows an emission band at 443 nm was bathochromically shifted to $\lambda_{max}$=448 nm, whereas the band at 546 nm underwent hypsochromic shift to $\lambda_{max}$= 529 nm (Fig. 3b) associated with a visually detectable change in solution from sky blue to dark green under UV lamp of 365 nm. In order to get an insight the association constant *Ka* of the **DTPDA**-$Pb^{2+}$ complex, the Benesi–Hildebrand equation was employed.

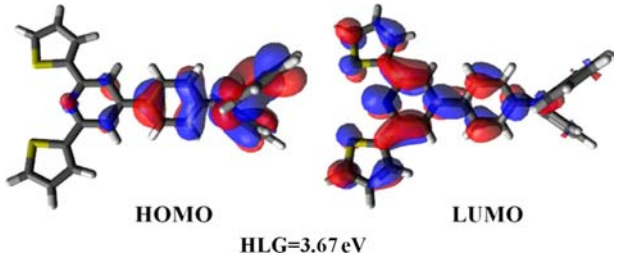


**Fig. 1.** Computational analysis of HOMO and LUMO levels of **DTPDA**.

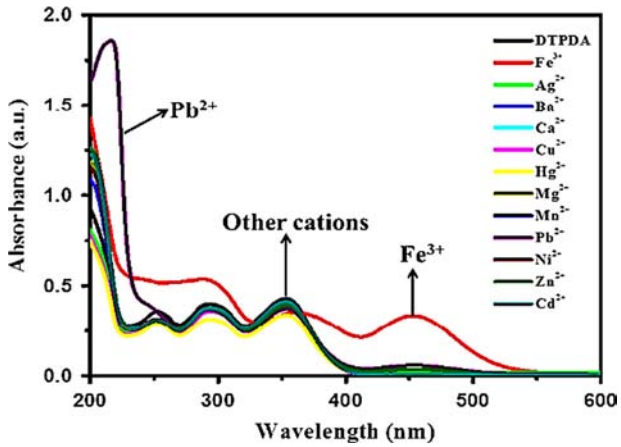


**Fig. 2.** Changes in UV–vis spectrum of **DTPDA** ($8\times10^{-5}$ M) upon addition of 10 equiv. of different metal cations in $CH_3CN$.

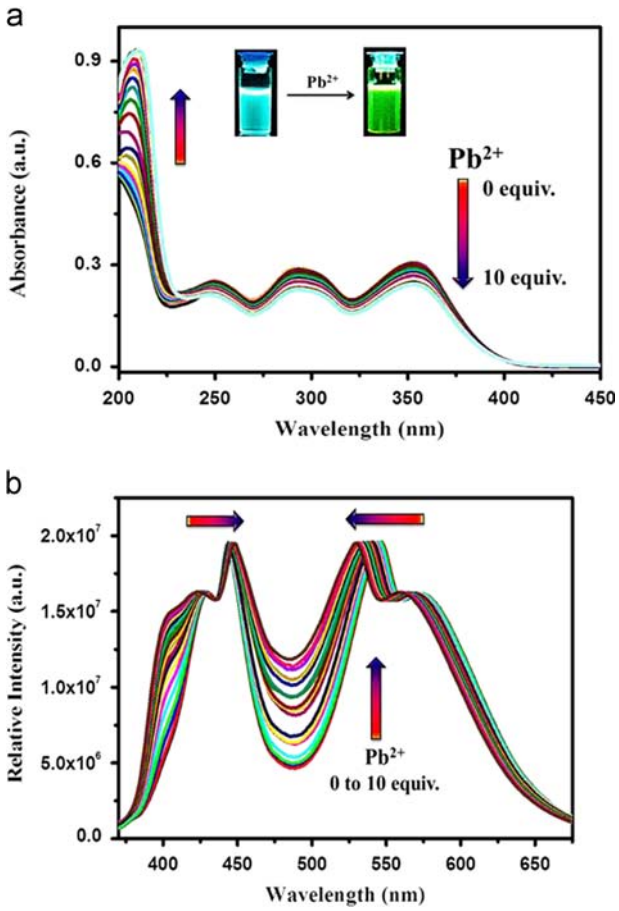


**Fig. 3.** (a) UV–vis and (b) Fluorescence spectra ($\lambda_{ex}$=350 nm) of **DTPDA** ($5\times10^{-5}$ M) in $CH_3CN$ upon addition of 0–10 equiv. of $Pb^{2+}$ ions ($2\times10^{-4}$ M). Inset of (a) shows naked eye visualisation of **DTPDA** upon addition of $Pb^{+2}$ at $\lambda_{ex}$=350 nm. (For interpretation of the references to color in this figure legend, the reader is referred to the web version of this article.)

It was evaluated graphically by plotting **DTPDA**/ΔA against **DTPDA**/[$Pb^{2+}$] (Fig. S4). The data linearly fitted to the Benesi–Hildebrand equation and the association constant (*Ka*) for $Pb^{2+}$ binding in **DTPDA** was determined to be $3.48 \times 10^4\ M^{-1}$. The detection limit of the **DTPDA**-$Pb^{2+}$ complex was determined from the plot of absorption intensity at 209 nm as a function of the concentration of $Pb^{2+}$ and found that **DTPDA** has detection limit to be 0.18 μM for the $Pb^{2+}$ ion (Fig. S5).

The changes in absorbance spectra of **DTPDA** were monitored upon gradual addition of $Fe^{3+}$ ions, the absorption band at 352 nm was bathochromic shifted to 364 nm ($\Delta\lambda_{max}=12$ nm) along with the formation of a new absorption peak at 453 nm (Fig. 4a). A new absorption band at 453 nm appeared and then stabilized above 1 equiv. while, absorption band at 364 nm was found to decrease in intensity with a small red-shift. The bands with a maximum at 200 nm and 300 nm increases with increase in concentration of $Fe^{+3}$ ions. The linear increase in absorption intensity at 452 nm was plotted against number of equivalent of $Fe^{3+}$ indicates a 1:1 stoichiometry for **DTPDA** and $Fe^{3+}$ complex (Fig. S6). The complex formation of **DTPDA**•$Fe^{3+}$ was also investigated by fluorescence spectroscopy. The emission spectrum of complex (Fig. 4b), initially shows slight red-shift at 443 nm and blue-shift at 543 nm ($\lambda_{ex}=350$ nm) underwent merging of both peaks and broadened at 489 nm. Furthermore, upon increasing concentration of $Fe^{3+}$, up to 10 equiv. results decrease in peak intensity. These spectral changes were associated with a colorimetric detectable change in solution fluorescence from sky blue to dark green (Fig. S1) under UV–vis ($\lambda_{ex}=365$ nm). We assume that the **DTPDA**•$Fe^{3+}$ complex

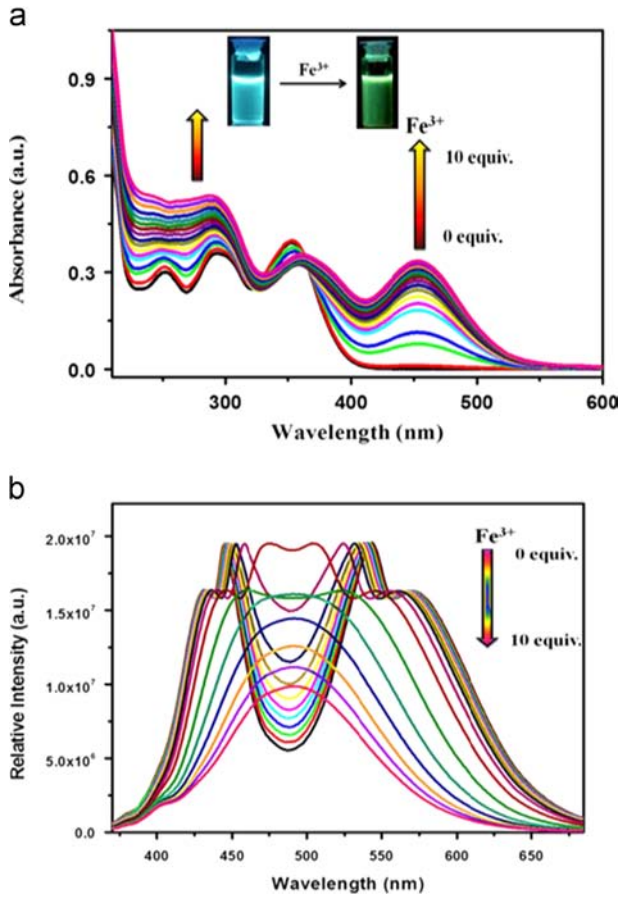


**Fig. 4.** (a) UV–vis and (b) fluorescence spectra ($\lambda_{ex}=350$ nm) of **DTPDA** ($5 \times 10^{-5}$ M) in $CH_3CN$ upon addition of varying equiv. of $Fe^{3+}$ ions ($2 \times 10^{-4}$ M). Inset of (a) shows naked eye visualisation of **DTPDA** upon addition of $Fe^{3+}$ at $\lambda_{ex}=350$ nm. (For interpretation of the references to color in this figure legend, the reader is referred to the web version of this article.)

formation played an important role in the modification of the ICT process from the donor diphenylamine unit to the acceptor end and this is supported by the sharp change in colour (observed both visually) and in their UV–vis and fluorescence spectra).

The association constant *Ka* of the **DTPDA**•$Fe^{3+}$ complex was evaluated by linearly fitted data obtained from plotting of **DTPDA**/ΔA against **DTPDA**/[$Fe^{3+}$] to the Benesi–Hildebrand equation (Fig. S7). The association constant (*Ka*) for $Fe^{3+}$ binding in **DTPDA** was determined to be $1.33 \times 10^4\ M^{-1}$ and the calculated detection limit of **DTPDA**.$Fe^{3+}$ complex to be 0.38 μM for $Fe^{3+}$ ion (Fig. S8).

### 3.3. Comparative binding studies of cations

The competitive binding studies of **DTPDA** with $Pb^{2+}$ and $Fe^{3+}$ were also carried out in the presence of 1 equiv. other cations such as $Ag^{+}$, $Ba^{2+}$, $Ca^{2+}$, $Cu^{2+}$, $Hg^{2+}$, $Mg^{2+}$, $Mn^{2+}$, $Ni^{2+}$, $Zn^{2+}$ and $Cd^{2+}$. The absorption band intensities of **DTPDA** did not change upon addition of 1 equiv. of any of these cations. However, addition of $Pb^{2+}$ to **DTPDA** in presence of these individual cations resulted in a remarkable enhancement in the absorption band at 209 nm intensity indicating the excellent selectivity and sensitivity of the receptor towards $Pb^{2+}$ (Fig. 5a). Furthermore, the selectivity and sensitivity of the receptor **DTPDA** was also tested towards $Fe^{3+}$. It should be noted that an increase in the intensity of absorbance peak at 453 nm from **DTPDA** was observed in the presence of other cations for $Fe^{3+}$ binding (Fig. 5b). Thus, **DTPDA** binds $Fe^{3+}$ selectively in presence of other cations Fig. 6).

Thus, compound **DTPDA** has a capability to recognise both Pb (II) and Fe(III) ions. This compound show absorption response as decrease in peak intensity in case of $Pb^{2+}$ (Fig. 3a) and increase in absorption peaks for $Fe^{3+}$ (Fig. 4a). This is because **DTPDA** does not show same binding mode to these two cationic species. These results again support the proposed mechanism.

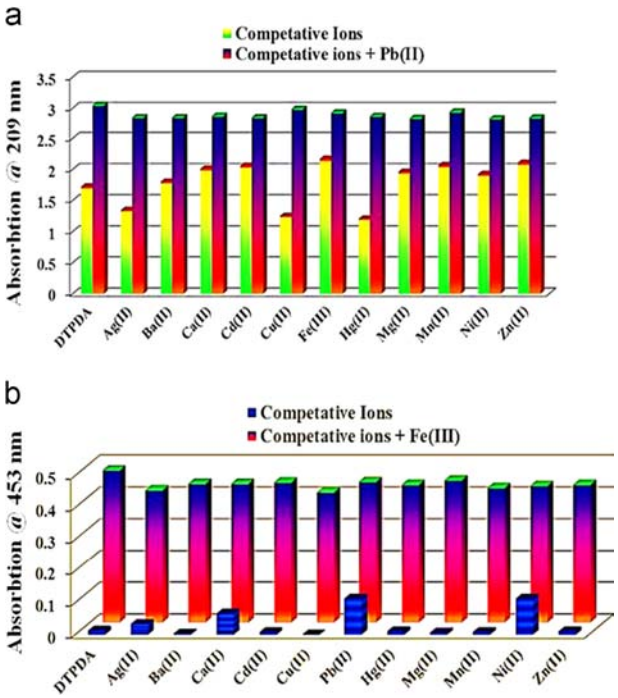


**Fig. 5.** Competitive responses of **DTPDA** and (a) **DTPDA**-$Pb^{2+}$ complex at 209 nm, (b) **DTPDA**-$Fe^{3+}$ complex at 453 nm in absorption intensity with different metal cations. The above study of receptor **DTPDA** with various cations using naked-eye, UV–vis, fluorescence spectroscopic techniques indicate that receptor **DTPDA** exhibits selective sensing for $Pb^{+2}$ and $Fe^{+3}$ in organic solvents. The plausible structure of the complex formation between receptor **DTPDA** and cation is as depicted in Fig. 6.

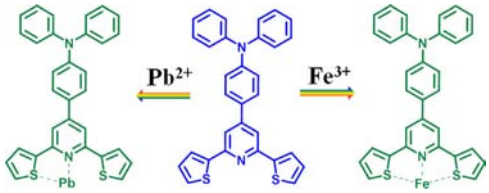


**Fig. 6.** The plausible structure of the complex resulted between receptor DTPDA and cation (DTPDA-$Pb^{2+}$ and DTPDA-$Fe^{3+}$ complex) ion.

## 4. Conclusions

In summary, we have demonstrated micromolar level detection $Pb^{2+}$ and $Fe^{3+}$ ions in acetonitrile utilising a donor–acceptor **DTPDA** receptor in both optical and calorimetric detection. The receptor exhibited selective and excellent probe for detection of $Pb^{2+}$ and $Fe^{3+}$ binding selectivity over other cations ($Ag^{+}$, $Ba^{2+}$, $Ca^{2+}$, $Cu^{2+}$, $Hg^{2+}$, $Mg^{2+}$, $Mn^{2+}$, $Ni2^{+}$, $Zn^{2+}$ and $Cd^{2+}$).

## Acknowledgements

Dr. Sid. V. Bhosale would like to thank the DAE-BRNS (Project Code: 37(2)/14/08/2014-BRNS), Mumbai, India for financial support. Dr. Avinash L. Puyad acknowledges use of the High Performance Computing Facility (Linux Cluster) and Gaussian 09 procured under the DST-FIST Scheme (Sanction No. FS/FST/PSI-018/2009). S.V. B. (RMIT) acknowledges financial support from the Australian Research Council under a Future Fellowship Scheme (FT110100152) and the School of Applied Sciences (RMIT University) for the facilities.

## Appendix A. Supporting information

Supplementary data associated with this article can be found in the online version at http://dx.doi.org/10.1016/j.talanta.2014.06.064.

## References

[1] A.P. de Silva, H.Q.N. Gunaratne, T. Gunnlaugsson, A.J.M. Huxley, C.P. McCoy, J. T. Rademacher, T.E. Rice, Chem. Rev. 97 (1997) 1515–1566.
[2] J.J. Lavigne, E.V. Anslyn, Angew. Chem. Int. Ed. 40 (2001) 3118–3130.
[3] R. Martínez- Mánez, F. Sancenón, Chem. Rev. 103 (2003) 4419–4476.
[4] P.D. Beer, P.A. Gale, Angew. Chem. Int. Ed. 40 (2001) 486–516.
[5] T. Schrader, A.D. Hamilton, Functional Synthetic Receptors, Wiley-VCH, Weinheim, 2005.
[6] J.S. Lin-Fu, Lead Poisoning, A Century of Discovery and Rediscovery. In Human Lead Exposure, in: H.L. Needleman (Ed.), Boca Raton, FL, Lewis Publishing, 1992.
[7] Guidelines for Drinking Water Quality, second ed.; World Health Organization: Geneva, 2, 1996, 940.
[8] J. Wang, K. Pantopoulos, Biochem. J. 434 (2011) 365–381.
[9] G. Cairo, A. Pietrangelo, Biochem. J. 352 (2000) 241–250.
[10] N.C.N. Andrews, Engl. J. Med. 341 (1999) 1986–1995.
[11] M. Kumar, R. Kumar, V. Bhalla, Org. Lett. 13 (2011) 366–369.
[12] J.Y. Kwon, Y.J. Jang, Y.J. Lee, K.M. Kim, M.S. Seo, W. Nam, J.J. Yoon, J. Am. Chem. Soc. 127 (2005) 10107–10111.
[13] M. Kumar, R. Kumar, V. Bhalla, P.R. Sharma, T. Kaur, Y. Qurishi, Dalton Trans. 41 (2012) 408–412.
[14] F. Zapata, A. Caballero, A. Espinosa, A. Tárraga, P. Molina, Org. Lett. 10 (2008) 41–44.
[15] Y. Chen, J. Jiang, Org. Biomol. Chem. 10 (2012) 4782–4787.
[16] J. Park, Y. Kim, Analyst 137 (2012) 3246–3248.
[17] K.M. Lee, X. Chen, W. Fang, J.-M. Kim, J. Yoon, Macromol. Rapid Commun. 32 (2011) 497–500.
[18] Y. Lin, X. Zhan, Chem. Soc. Rev. 41 (2012) 4245–4272.
[19] L. Duan, L. Hou, T.W. Lee, J. Qiao, D. Zhang, G. Dong, L. Wang, Y.J. Qiu, Mater. Chem. 20 (2010) 6392–6407.
[20] E. Ripaud, Y. Olivier, P. Leriche, J. Cornil, J. Roncali, J. Phys. Chem. B 115 (2011) 9379–9386.
[21] J. Kwon, W. Lee, J.-Y. Kim, S. Noh, C. Lee, J.-I. Hong, New J. Chem. 34 (2010) 744–749.
[22] G. Qian, Z.Y. Wang, J. Mater. Chem. 19 (2009) 522–530.
[23] X. Zhang, M. Kang, H.-A. Choi, J.Y. Jung, K.M.K. Swamy, S. Kim, D. Kim, J. Kim, C. Lee, J. Yoon, Sens. Actuators, B 192 (2014) 691–696.
[24] S.C. Luo, J. Sekine, B. Zhu, H. Zhao, A. Nakao, H. Yu, ACS Nano 6 (2012) 3018–3026.
[25] W. Xu, B. Peng, J. Chen, M. Liang, F. Cai, J. Phys. Chem. C 112 (2008) 874–880.
[26] B. Liu, Y. Bao, F. Du, H. Wang, J. Tian, R. Bai, Chem. Commun. 47 (2011) 1731–1733.
[27] F. Kröhnke, Synthesis (1976) 1–24.
[28] L.-X. Zhao, T.S. Kim, S.-H. Ahn, T.-H. Kim, E.-K. Kim, W.-J. Cho, H. Choi, C.-S. Lee, J.A. Kim, T.C. Jeong, C.-J. Chang, E.-S. Lee, Bioorg. Med. Chem. Lett. 11 (2001) 2659–2662.
[29] J. Hovinen, V.-M. Mukkala, H. Hakala, J. Peuralahti, Novel chelating agents and chelates and their use. U.S. Patent 2005/0084451 A1, April 21, 2005.
[30] M.J. Frisch, et al., Gaussian 09, Revision.C.01, (2009), Gaussian Inc., Wallingford CT, 2009.
[31] Avogadro: an open-source molecular builder and visualization tool. Version 1.1.0. ⟨http://avogadro.openmolecules.net/⟩.
[32] M.D. Hanwell, D.E. Curtis, D.C. Lonie, T. Vandermeersch, E. Zurek, G. R. Hutchison, J. Cheminform. 4 (2012) 1–17.
[33] S. Tao, Y. Zhou, C.–S. Lee, S.–T. Lee, D. Huang, X. Zhang, J. Phys. Chem. C 112 (2008) 14603–14606.
[34] S.J. Higgins, T.J. Poundsa, P.A. Christensen, J. Mater. Chem. 11 (2001) 2253–2261.